Controlling toroidal moments by crossed electric and magnetic fields

M. Baum,[1] K. Schmalzl,[2] P. Steffens,[3] A. Hiess,[3,*] L. P. Regnault,[4] M. Meven,[5] P. Becker,[6] L. Bohatý,[6] and M. Braden[1,†]

[1]*II. Physikalisches Institut, Universität zu Köln, Zülpicher Strasse 77, 50937 Köln, Germany*
[2]*Institut für Festkörperforschung, Forschungszentrum Jülich GmbH, JCNS at ILL, 38042 Grenoble Cedex 9, France*
[3]*Institut Laue-Langevin, BP 156, 38042 Grenoble Cedex 9, France*
[4]*Institut Nanosciences et Cryogénie, CEA Grenoble, 38054 Grenoble Cedex 9, France*
[5]*RWTH Aachen – JCNS Outstation at FRM II, Lichtenbergstr. 1, 85748 Garching, Germany*
[6]*Institut für Kristallographie, Universität zu Köln, Greinstrasse 6, 50939 Köln, Germany*

(Received 24 July 2012; revised manuscript received 25 June 2013; published 15 July 2013)

The control of ferroelastic, ferroelectric, and ferromagnetic domains through the corresponding fields has led to numerous applications taken for granted nowadays. Ferrotoroidal order on the other hand has been less explored due to its more complex character and due to the peculiar field needed to control it. $LiFeSi_2O_6$ exhibits a ferrotoroidal order that is particularly simple to analyze. By performing neutron-diffraction experiments with spherical polarization analysis we show that crossed electric and magnetic fields allow us to control ferrotoroidal moments.

DOI: 10.1103/PhysRevB.88.024414 PACS number(s): 75.85.+t, 75.10.−b, 75.25.−j, 75.60.−d

It would be hard to imagine the modern world without the ability to pole and control ferroic order. Ferromagnetic domains form the basis of today's most efficient data storage and there are numerous applications for ferroelectricity and ferroelasticity as well. Considering the impact of the inversion of time and of space ferroic order can be easily classified:[1,2] ferroelastic order is invariant against time and space inversion (++); ferroelectricity is invariant against time inversion but changes sign upon space inversion (+−) and ferromagnetism is time-odd and space-even (−+). The ferroic order, which changes sign upon both time and space inversion (−−) and which is invariant against the concomitant inversion of both, is the ferrotoroidal order.[2] A toroidal moment can arise either by head-to-tail arrangement of local moments or by orbital currents. Ferrotoroidal order results from spontaneous parallel alignments of the toroidal moments. For local moments, the toroidal moment of a cell can be obtained by $\boldsymbol{t} = \frac{1}{2}\sum_i \boldsymbol{r}_i \times \boldsymbol{m}_i$ with $\boldsymbol{r}_i$ and $\boldsymbol{m}_i$ being the space coordinate and the magnetic spin or orbital moment of the ith atom.[3] The toroidization is given by $\boldsymbol{T} = \frac{1}{V}\boldsymbol{t} = \frac{1}{2V}\sum_i \boldsymbol{r}_i \times \boldsymbol{m}_i$ with V the volume of the unit cell and the sum running over a primitive basis. The value of toroidization, however, is not uniquely defined but depends on the basis chosen for the sum similar to the case of the ferroelectric polarization.[3] Ferrotoroidal order has regained interest quite recently due to its close relation with the linear magnetoelectric effect.[1,2] In the presence of ferrotoroidal order there will be asymmetric components in the magnetoelectric tensor as it can be seen from the relation between the ferroelectric polarization and magnetic field: $\boldsymbol{P}_{\mathrm{FE}} \propto \boldsymbol{T} \times \boldsymbol{H}$. The field directly coupled to ferrotoroidal order is an inhomogeneous magnetic field with a nonvanishing curl that may align with the ring of magnetic moments. Such a magnetic field, however, can only exist in the presence of electric currents. On the other hand one may use crossed magnetic and electric fields to pole the ferrotoroidal moments profiting of the nondiagonal terms in the magnetoelectric tensor. We will show that with such fields it is indeed possible to pole ferrotoroidal domains.

$LiFeSi_2O_6$ is a member of the pyroxene family recently shown to exhibit interesting magnetoelectric and multiferroic properties (see Fig. 1).[4] In this material class chains of edge-sharing MeO_6 octahedra (Me = Fe, Cr, ...) are connected through SiO_4 or GeO_4 tetrahedra chains. Due to the edge-sharing of the octahedra the nearest-neighbor Me-Me interaction is considerably weakened in comparison to a straight Me-O-Me bond, therefore, several other intra- and interchain interaction parameters are comparable in size and the system becomes frustrated.[5] While $NaFeSi_2O_6$ (natural crystals) exhibits a ferroelectric polarization coupled with incommensurate magnetic ordering at zero magnetic field,[4] $LiFeSi_2O_6$ shows a single magnetic transition into a commensurate magnetic phase.[6] There is no spontaneous ferroelectric polarization at zero magnetic field but sizable electric polarization is induced by finite magnetic fields in $LiFeSi_2O_6$. Most interestingly there are asymmetric off-diagonal components in the magnetoelectric tensor.[7] The crystal structures of $NaFeSi_2O_6$ and $LiFeSi_2O_6$ are monoclinic and at room temperature both materials crystallize in the same space group ($C2/c$). However, $LiFeSi_2O_6$ exhibits at $T_S = 229$ K a structural phase transition that is characterized by a loss in translation symmetry (space group $P2_1/c$; lattice parameters $a = 9.62$ Å, $b = 8.66$ Å, $c = 5.26$ Å, $\beta = 110.0°$).[8,9] This structural distortion is induced by the smaller ionic radius of Li and can be understood as a twisting of the SiO_4 chains which diminishes the Li-O distances. Most important are the displacements observed for the magnetic Fe ions. In the primitive cell of the $P2_1/c$ low-temperature phase there are four Fe sites belonging to two FeO_6 chains running along the monoclinic c direction; see Fig. 2 and the Appendix. The symmetry reduction from $C2/c$ to $P2_1/c$ allows for a displacement $\boldsymbol{r}_{ac}$ of the Fe atoms within the ac plane; these displacements are parallel within a single FeO_6 chain and antiparallel for the two chains in the primitive cell.

There have been contradictory reports on the magnetic structure of $LiFeSi_2O_6$ based on powder neutron diffraction;[8,9] our own single-crystal diffraction experiment on the HEIDI

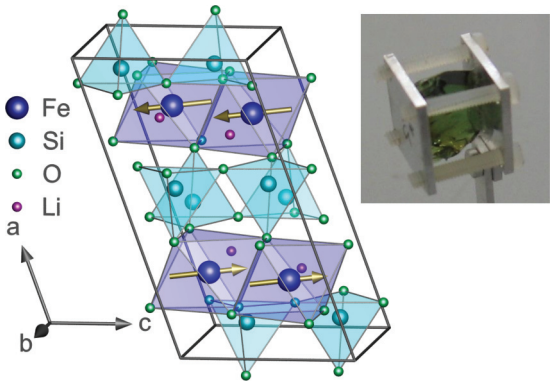

FIG. 1. (Color online) Left: Structure of $LiFeSi_2O_6$ indicating the Fe, Si, O, and Li positions. Right: Photo of the sample crystal. The distance between the aluminium plates is 8 mm. The plates are fixed with nylon screws, additionally the sample is glued to the plates. The high voltage was applied to the plates yielding a nearly homogeneous magnetic field in the sample volume.

diffractometer at FMR II identifies $P2_1/c'$ (point group $2/m'$) as the most probable magnetic space group in $LiFeSi_2O_6$ (see the Appendix) consistent with the more recent powder study. Only this magnetic group is in accordance with the finite off-diagonal magnetoelectric coefficients α_{31} and α_{13}.[7,10] Symmetry analysis shows that a collinear arrangement of magnetic moments $\boldsymbol{m}_{ac}$ in the ac plane is coupled with a b component leading to a canted antiferromagnetic structure. The b component, however does not contribute to the ferrotoroidal moment and will be ignored in the following. The moments in the ac plane are parallel within a chain and antiparallel in between. The alignment of the in-plane moments is thus the same as that of the the structural displacements of the Fe ions, as illustrated in Fig. 2. Let us first calculate the toroidization for a vanishing structural distortion. In space group $C2/c$ there is an inversion center connecting the two Fe sites in a single chain (sites 1 and 4, Fig. 2). Since the two moments are parallel toroidal contributions cancel out.

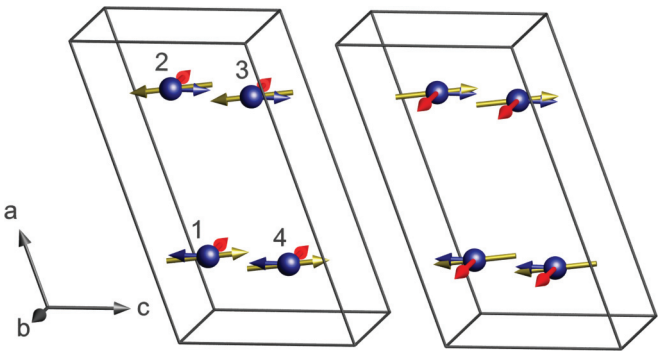

FIG. 2. (Color online) Structural distortions and magnetic moments in $LiFeSi_2O_6$; only the Fe ions in a primitive cell are shown. The structural displacements with respect to the high-temperature phase are shown by blue arrows (enlarged by a factor 10) and the magnetic moment by yellow arrows; the contribution to the total toroidal moment of each ion is indicated by red arrows. The left and right panels show the two toroidal domains which are characterized by nearly antiparallel and nearly parallel alignment of the structural displacement and the magnetic moment, respectively.

The same inversion center also connects site 2 with site 3 translated by one negative a lattice constant; since also these two sites exhibit parallel magnetic components the toroidal moments cancel out again. Without the structural distortion the toroidal moment thus vanishes. As illustrated in Fig. 2, the structural displacements $\boldsymbol{r}_{ac}$ and the magnetic moments have the same relative phases at the four Fe sites, therefore the toroidal components arising from the shift of the four atoms add. For a finite structural displacement we thus easily obtain $\boldsymbol{T} = \frac{2}{V}\boldsymbol{r}_{ac} \times \boldsymbol{m}_{ac}$ which points along the monoclinic b axis. With the crystal and magnetic structural parameters we obtain $|\boldsymbol{T}| = 0.000\,25(3)\mu_B/\text{Å}^2$ which is a small value due to the coupling with the weak nuclear superstructure.

The toroidization in $LiFeSi_2O_6$ corresponds to the product of the order parameters of the structural and the magnetic phase transitions, which are proportional to the components of the structural displacement and to the magnetic moment, respectively. The two toroidal domains with toroidization parallel and antiparallel to the b axis result from nearly parallel or nearly antiparallel alignment of magnetic moment and structural displacement. Note that the structural transition only results in 180° domains associated with the sign of the structural order parameter. The same holds for the magnetic transition. Therefore one can identify four different domains with magnetic and structural phases of (0°,0°), (0°,180°), (180°,0°), and (180°,180°), respectively. From these the first and the last together form the up-toroidization domain, while the second and the third form the down-toroidization domain. Toroidal and magnetic domains are therefore not identical, as is the case in $LiCoPO_4$,[1,11] rendering $LiFeSi_2O_6$ an even more interesting material.

Simple diffraction experiments sense the square of nuclear or structural order parameters so that information about the phases between these two or the phases of the nuclear, F_N, and the magnetic structure factors, $\boldsymbol{M}$, themselves are lost. However, polarized neutron scattering gives direct access to the interference between nuclear and magnetic structure factors and therefore the product of the phases of F_N and $\boldsymbol{M}$ can be determined.[12–14] As shown above, this product just corresponds to the ferrotoroidal moment. The centrosymmetric nuclear structure and the anticentrosymmetric magnetic structure (symmetry element $\bar{1}'$) facilitate the calculation, as F_N is real and $\boldsymbol{M}$ is purely imaginary. For the nuclear part this just corresponds to the well-known rule, and for the magnetic part the antiparallel alignment of moments at (x,y,z) and $(\bar{x},\bar{y},\bar{z})$ just leads to the cancellation of the cosine terms and thus to a purely imaginary magnetic structure factor. We use the common coordinate system in spherical neutron polarization studies with the x axis along the scattering vector, the y axis in the scattering plane perpendicular to x, and the z axis perpendicular to the scattering plane.[14] The measurements have been performed in the a^*b^* scattering plane at $\boldsymbol{Q} = (3,0,0)$ which is a nuclear and a magnetic superstructure reflection. Note that this reflection is extinct in the high-temperature nuclear phase due to its C centering. At this reflection the b component of the magnetic order does not contribute, therefore $\boldsymbol{M}$ only has a finite z component $M_z = im_z$ with m_z being real. (Note that M_x is always zero in neutron diffraction as only magnetic components perpendicular to the scattering vector $\boldsymbol{Q}$ contribute.)

Spherical polarization analysis allows one to measure the rotation of polarization between the incoming, $\boldsymbol{P}$, and outgoing, $\boldsymbol{P}'$, beam.[14] Since there are no chiral terms in the magnetic structure of $LiFeSi_2O_6$ and since the product $F_N \boldsymbol{M}$ has no real components, there are no contributions generating polarization in the outgoing beam for zero incoming polarization and it follows $\boldsymbol{P}' = \boldsymbol{\mathcal{P}}' \boldsymbol{P}$ with $\boldsymbol{\mathcal{P}}'$ being the polarization matrix. Consider the channel when the incoming neutron polarization is set along the y axis and when the outgoing polarization is measured for the x axis. As there are no chiral terms in the magnetic structure, the only term yielding x polarization is given by

$$\mathcal{P}'_{xy} = \frac{2\mathrm{Im}(F_N M_z^*)}{M^2 + F_N^2} = -\frac{2F_N m_z}{m_z^2 + F_N^2}. \quad (1)$$

Here Im describes the imaginary part and * is the complex conjugate. Since F_N is real and $\boldsymbol{M}$ purely imaginary, $\mathrm{Im}(F_N M_z^*) = -F_N m_z$ is a real number that is proportional to the total toroidization of the sample at constant temperature. We wish to emphasize that the neutron polarization in this channel thus probes the sign and the size of the toroidization averaged over the sample crystal. This nondiagonal neutron-polarization channel is thus a direct measure of the toroidization. Entering the crystal and magnetic structure of $LiFeSi_2O_6$ at 10 K yields a polarization of $\mathcal{P}'_{xy} = \pm 0.077$ for the two monodomain states with opposed directions of the toroidization. In the same way one can calculate the expected polarization in the inverted channel, $\mathcal{P}'_{yx} = \mp 0.077$. The full polarization matrix $\boldsymbol{\mathcal{P}}'$ can be easily calculated in this case as most contributions vanish for $\boldsymbol{Q} = (3,0,0)$:[14]

$$\boldsymbol{\mathcal{P}}' = \begin{pmatrix} \frac{F_N^2 - m_z^2}{F_N^2 + m_z^2} & -\frac{2F_N m_z}{F_N^2 + m_z^2} & 0 \\ \frac{2F_N m_z}{F_N^2 + m_z^2} & \frac{F_N^2 - m_z^2}{F_N^2 + m_z^2} & 0 \\ 0 & 0 & \frac{F_N^2 + m_z^2}{F_N^2 + m_z^2} \end{pmatrix} = \begin{pmatrix} -0.997 & -0.077 & 0 \\ 0.077 & -0.997 & 0 \\ 0 & 0 & 1 \end{pmatrix}. \quad (2)$$

The $\boldsymbol{\mathcal{P}}'$ matrix for the domain with opposed toroidal moment, which corresponds to a 180° phase shift either in the nuclear or in the magnetic structure, differs just in the exchange of the xy and yx components. In contrast, the domain with 180° phase shifts in both nuclear and magnetic structure yields the identical matrix. Note that the large beam polarization in all diagonal channels results from the much stronger magnetic scattering at $\boldsymbol{Q} = (3,0,0)$.

Unfortunately spherical polarization analysis cannot be performed with a magnetic field at the sample position, as this would interfere with the neutron polarization. We have used the CRYOPAD setup in which superconducting shields expel the magnetic field.[14] The poling of the ferrotoroidal moment thus cannot be studied *in situ*, but the sample needs to be cooled in crossed magnetic and electric fields below the magnetic transition outside of the CRYOPAD. The cold sample can then be inserted into the CRYOPAD and the analysis of the toroidal moment can be made. This procedure is identical to that applied to obtain a magnetic monodomain state in Cr_2O_3 (Ref. 15) and in $MnPS_3$ (Ref. 16) which was proposed as a candidate for ferrotorodicity. The neutron-diffraction experiments were realized on the cold triple-axis spectrometer IN14 at the Institut Laue Langevin. The neutron wave vector was set to $k = 1.5$ Å^{-1}. An electric field was applied by inserting the plate-shaped single crystalline sample of synthetic $LiFeSi_2O_6$ (plate normal b parallel to the aluminium plates, c axis vertical) between two thin aluminium plates (8 mm apart) that are nearly transparent for neutrons. The sample was glued in between these plates, which were further stabilized by nylon screws; see Fig. 1. The sample with the capacitor was mounted in a cryostat with a sufficiently thin tail to enter both the CRYOPAD setup and an external magnet. The sample was cooled outside the spectrometer in an electric field of 2.5 kV/cm applied along a^* while a magnetic field of $\mu_0 \boldsymbol{H} = 1$ T was applied along the crystallographic c axis. Thereby cooling in crossed fields with finite $\boldsymbol{E} \times \boldsymbol{H}$ parallel to the direction of the toroidization (i.e., b direction) was achieved. At a temperature of 10 K both fields were removed and the cold sample was transferred to the spectrometer and the CRYOPAD setup.

The first measurement of the neutron polarization matrix at the (3,0,0) reflection after the above-described cooling in crossed fields $(+\boldsymbol{E}) \times (+\boldsymbol{H})$ yields

$$\boldsymbol{\mathcal{P}}'_{\mathrm{exp}} = \begin{pmatrix} -1.00(1) & -0.07(1) & 0.01(1) \\ 0.06(1) & -1.00(1) & 0.01(1) \\ 0.01(1) & 0.02(1) & 1.00(1) \end{pmatrix}. \quad (3)$$

Errors in the nondiagonal channels are not due to statistics but reflect the precision of polarization control. By analyzing a purely structural reflection we may estimate the precision in these off-diagonal channels to ±0.01. The flipping ratio measured on a Bragg peak in the paramagnetic phase amounts to 25.

The good agreement between the calculated and experimental polarization matrix unambiguously shows that it is possible to pole the toroidal domains in $LiFeSi_2O_6$ by applying crossed fields. A measurement of the off-diagonal channels after cooling without applied fields did not result in significant polarization values.

We repeated the measurement by reversing the magnetic field only, $(+\boldsymbol{E}) \times (-\boldsymbol{H})$, and obtained $\mathcal{P}'_{xy} = 0.04(1)$ and $\mathcal{P}'_{yx} = -0.04(1)$ which perfectly agrees with the expected inversion of the toroidization although the poling appears to be slightly less perfect in this run. These two experiments unambiguously show that it is possible to control the ferrotoroidal moment by crossed fields similar to the usual control of ferroic order.

TABLE I. Neutron polarization as function of different cooling fields. The sample was cooled from 33 to 10 K in the particular field. $E = \pm 2.5$ kV/cm, $\mu_0 H = \pm 1$ T.

E	H	P'_{xy}	P'_{yx}
+	+	−0.07(1)	0.06(1)
+	−	0.04(1)	−0.04(1)
−	−	−0.06(1)	0.05(1)
+	0	0.00(1)	−0.01(1)
−	0	−0.00(1)	−0.01(1)
0	−	0.01(1)	−0.02(1)

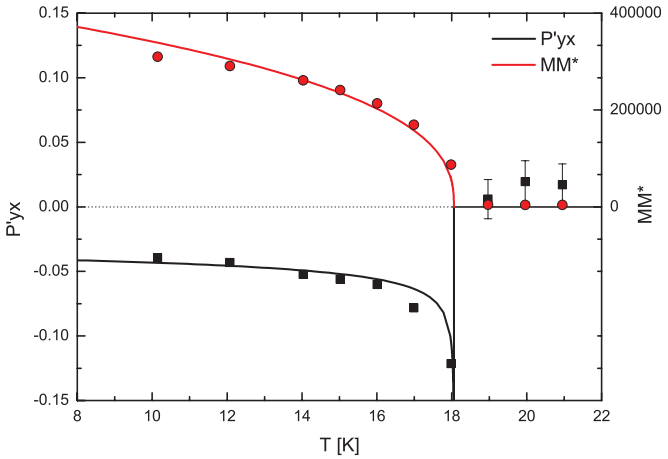

FIG. 3. (Color online) Temperature dependence of the magnetic Bragg intensity $\boldsymbol{M}\ \boldsymbol{M}^*$ at $\boldsymbol{Q} = (3,0,0)$ and that of the neutron polarization in the $\mathcal{P}'_{yx}$ channel as described by Eq. (1).

Our experiment only senses the product $F_N\, m_z$ and, therefore, we may not conclude whether the change in toroidicity arises from inversion of the magnetic moment or from inversion of structural distortions. However, the high structural transition temperature, much above our poling procedure, renders a control of structural domains less likely.

The next experiment was done with both fields being reversed, $(-\boldsymbol{E}) \times (-\boldsymbol{H})$, yielding $\mathcal{P}'_{xy} = -0.06(1)$ and $\mathcal{P}'_{yx} = 0.05(1)$, which correspond as expected to the same direction of toroidization as for the $(+\boldsymbol{E}) \times (+\boldsymbol{H})$ run. We furthermore verified that it is not possible to pole the toroidization in $LiFeSi_2O_6$ by applying just one, either magnetic or electric, field. This, further, underlines the special character of the toroidal material in comparison to magnetoelectric multiferroics. In the toroidal material both fields are needed to pole the ferroic state, which is just a consequence of the linear magnetoelectric effect. The experimental data are summarized in Table I.

Figure 3 shows the temperature dependence of the magnetic Bragg-peak intensity at $\boldsymbol{Q} = (3,0,0)$, $\boldsymbol{M}\ \boldsymbol{M}^* = m_z^2$, compared to that of the neutron polarization in the yx channel, $\mathcal{P}'_{yx}$. Obviously the two quantities do not exhibit the same temperature dependence. While the magnetic Bragg intensity just corresponds to the expected power-law temperature dependence of the square of the magnetic moment, the polarization exhibits a maximum in absolute size close to the magnetic transition. This can be easily understood by analyzing Eq. (1). $|\mathcal{P}'_{yx}|$ is proportional to $\frac{|F_N\, m_z|}{F_N^2+m_z^2}$. By fitting the temperature-independent value of F_N^2 which is constant in this temperature range, and assuming $m_z^2 \propto (1 - \frac{T}{T_N})^{2\beta}$,[17] both temperature dependencies can be simultaneously described, $T_N = 18.1$ K and $\beta = 0.19$. The good agreement underlines that the polarization in this channel arises from nuclear-magnetic interference and thus from the toroidization. The poling of the toroidization is fully comparable to the poling of the multiferroic state by an electric field,[18–20] which has been reported prior to the hysteresis loops at constant temperature.[21–23]

In conclusion, we have shown that it is possible to control toroidal domains by crossed electric and magnetic field with $\boldsymbol{E} \times \boldsymbol{H}$ aligned along the direction of toroidization. Cooling in such fields results in a nearly monodomain toroidal state, whereas cooling in zero fields or with only a single finite electric or magnetic component results in an equal distribution of toroidal domains.

This work was supported by the Deutsche Forschungsgemeinschaft through the Sonderforschungsbereich 608. We thank the D3 and SANE teams at ILL for their technical support required for this experiment.

TABLE II. The magnetic space group is $P2_1/c'$. Magnetic moment at 10 K: $(u,v,w) = [0.58(8),\ 0.69(3),\ 3.91(4)]\mu_B$, $|\boldsymbol{m}| = 3.81(3)\mu_B$.

Fe-site	Element	Symm. op.	Magn. moment
1	1	x,y,z	u,v,w
2	2_1	$\bar{x},y+\frac{1}{2},\bar{z}+\frac{1}{2}$	$\bar{u},v,\bar{w}$
3	$\bar{1}'$	$\bar{x},\bar{y},\bar{z}$	$\bar{u},\bar{v},\bar{w}$
4	c'	$x,\bar{y}+\frac{1}{2},z+\frac{1}{2}$	$u,\bar{v},w$

TABLE III. Structural parameters of $LiFeSi_2O_6$ at 20 K. $R_{F^2} = 5.0\%$, $R_{wF^2} = 7.8\%$, $R_F = 4.7\%$.

Atom	x	y	z	U_{iso} (Å^2)
Li	0.2486(5)	0.0066(5)	0.2376(8)	0.0104(9)
Fe	0.25014(10)	0.64815(10)	0.23462(17)	0.0080(2)
SiA	0.0478(2)	0.3395(2)	0.2783(4)	0.0072(4)
SiB	0.5485(2)	0.8392(2)	0.2509(4)	0.0079(4)
O1A	0.86710(16)	0.33254(17)	0.1634(3)	0.0083(3)
O1B	0.36712(16)	0.83405(17)	0.1338(3)	0.0086(3)
O2A	0.11589(15)	0.50899(17)	0.3098(3)	0.0092(3)
O2B	0.62236(15)	0.00355(17)	0.3543(3)	0.0094(3)
O3A	0.10887(16)	0.26758(16)	0.5840(3)	0.0087(3)
O3B	0.60519(16)	0.72238(18)	0.5108(3)	0.0086(3)

APPENDIX

Large single crystals of $LiFeSi_2O_6$ were grown from melt solvent of the system Li_2MoO_4-$LiVO_3$. The magnetic structure was determined at the HEIDI single-crystal diffractometer (FRM II) with $\lambda = 1.16$ Å. The crystal structure was determined in the paramagnetic phase at 20 K; 925 reflections

TABLE IV. Structural parameters of $LiFeSi_2O_6$ at 10 K. $R_{F^2} = 5.1\%$, $R_{wF^2} = 7.7\%$, $R_F = 4.7\%$.

Atom	x	y	z	U_{iso} (Å^2)
Li	0.2490(5)	0.0071(5)	0.2380(9)	0.0091(9)
Fe	0.25023(11)	0.64834(10)	0.23441(19)	0.0070(2)
SiA	0.0478(2)	0.3395(2)	0.2782(4)	0.0065(4)
SiB	0.5484(2)	0.8393(2)	0.2511(4)	0.0070(4)
O1A	0.86714(17)	0.33274(17)	0.1636(3)	0.0075(3)
O1B	0.36715(17)	0.83418(17)	0.1338(3)	0.0077(3)
O2A	0.11592(16)	0.50906(17)	0.3097(3)	0.0083(3)
O2B	0.62234(16)	0.00352(18)	0.3545(3)	0.0087(3)
O3A	0.10873(16)	0.26765(17)	0.5839(3)	0.0078(3)
O3B	0.60514(16)	0.72229(19)	0.5106(3)	0.0078(3)

were collected. In the magnetic phase at 10 K, 936 reflections were collected (magnetic and structural reflections superimpose). The data were numerically corrected for absorption and an extinction correction was applied in the refinement. The structure refinement was performed with the FULLPROF program.[24] The magnetic structure is presented in Table II and its caption. Structural results at two temperatures are given in Tables III and IV.

*Present address: ESS AB, Lund, Sweden.
†braden@ph2.uni-koeln.de

[1]H. Schmid, J. Phys.: Condens. Matter **20**, 434201 (2008).
[2]N. A. Spaldin, M. Fiebig, and M. Mostovoy, J. Phys.: Condens. Matter **20**, 434203 (2008).
[3]C. Ederer and N. A. Spaldin, Phys. Rev. B **76**, 214404 (2007).
[4]S. Jodlauk, P. Becker, J. A. Mydosh, D. I. Khomskii, T. Lorenz, S. V. Streltsov, D. C. Hezel, and L. Bohatý, J. Phys.: Condens. Matter **19**, 432201 (2007).
[5]S. V. Streltsov and D. I. Khomskii, Phys. Rev. B **77**, 064405 (2008).
[6]E. Baum, W. Treutmann, M. Behruzi, W. Lottermoser, and G. Amthauer, Z. Kristallogr. **183**, 273 (1988).
[7]S. Jodlauk, Ph.D. thesis, University of Cologne, 2009.
[8]G. J. Redhammer, G. Roth, W. Paulus, G. André, W. Lottermoser, G. Amthauer, W. Treutmann, and B. Koppelhuber-Bitschnau, Phys. Chem. Miner. **28**, 337 (2001).
[9]G. J. Redhammer, G. Roth, W. Treutmann, M. Hoelzel, W. Paulus, G. André, C. Pietzonka, and G. Amthauer, J. Solid State Chem. **182**, 2374 (2009).
[10]J.-P. Rivera, Ferroelectrics **161**, 165 (1994).
[11]B. B. Van Aken, J.-P. Rivera, H. Schmid, and M. Fiebig, Nature (London) **449**, 702 (2007).
[12]M. Blume, Phys. Rev. **130**, 1670 (1963).
[13]S. V. Maleev, V. G. Baŕyaktar, and P. A. Suris, Sov. Phys. Solid State **4**, 2533 (1963).
[14]P. J. Brown, in *Neutron Scattering from Magnetic Materials*, edited by T. Chatterji (Elsevier, New York, 2006), Chap. 5.
[15]P. J. Brown, J. B. Forsyth, and F. Tasset, J. Phys.: Condens. Matter **10**, 663 (1998).
[16]E. Ressouche, M. Loire, V. Simonet, R. Ballou, A. Stunault, and A. Wildes, Phys. Rev. B **82**, 100408 (2010).
[17]M. E. Fischer, Rep. Progr. Phys. **30**, 615 (1967).
[18]Y. Yamasaki, H. Sagayama, T. Goto, M. Matsuura, K. Hirota, T. Arima, and Y. Tokura, Phys. Rev. Lett. **98**, 147204 (2007).
[19]S. Seki, Y. Yamasaki, M. Soda, M. Matsuura, K. Hirota, and Y. Tokura, Phys. Rev. Lett. **100**, 127201 (2008).
[20]H. Sagayama, K. Taniguchi, N. Abe, T. H. Arima, M. Soda, M. Matsuura, and K. Hirota, Phys. Rev. B **77**, 220407(R) (2008).
[21]A. Poole, P. J. Brown, and A. S. Wills, J. Phys.: Conf. Ser. **145**, 012074 (2009).
[22]T. Finger, D. Senff, K. Schmalzl, W. Schmidt, L. P. Regnault, P. Becker, L. Bohatý, and M. Braden, Phys. Rev. B **81**, 054430 (2010).
[23]I. Cabrera, M. Kenzelmann, G. Lawes, Y. Chen, W. C. Chen, R. Erwin, T. R. Gentile, J. B. Leão, J. W. Lynn, N. Rogado, R. J. Cava, and C. Broholm, Phys. Rev. Lett. **103**, 087201 (2009).
[24]J. Rodríguez-Carvajal, http://www.ill.eu/sites/fullprof/.